Enhanced Piezo-Induced Photocatalytic Activity of $BaTiO_3/Cd_{0.5}Zn_{0.5}S$ S–Scheme Heterojunction for Water Pollution Remediation.

Tshepo T. Mohlala[a], Tunde L. Yusuf[b], Mike Masukume[c], Vincent Ojijo[c], Nonhlangabezo Mabuba[a,d*]

[a]*University of Johannesburg, Department of Chemical Science, Doornfontein Campus,*

Johannesburg, 2028, South Africa

[b]*Department of Chemistry, Faculty of Natural and Agricultural Sciences, University of Pretoria, Private Bag X20, Hatfield 0028, Pretoria, South Africa*

[c]*Council for Scientific and Industrial Research (CSIR), Pretoria Campus, Pretoria, 0001, South Africa*

[d]*Centre for Nanomaterial Science Research, Department of Chemical Sciences, Doornfontein Campus, Johannesburg, 2028, South Africa*

***Corresponding author**: Nonhlangabezo Mabuba **Email**: nmabuba@uj.ac.za

SUPPLEMENTARY INFORMATION

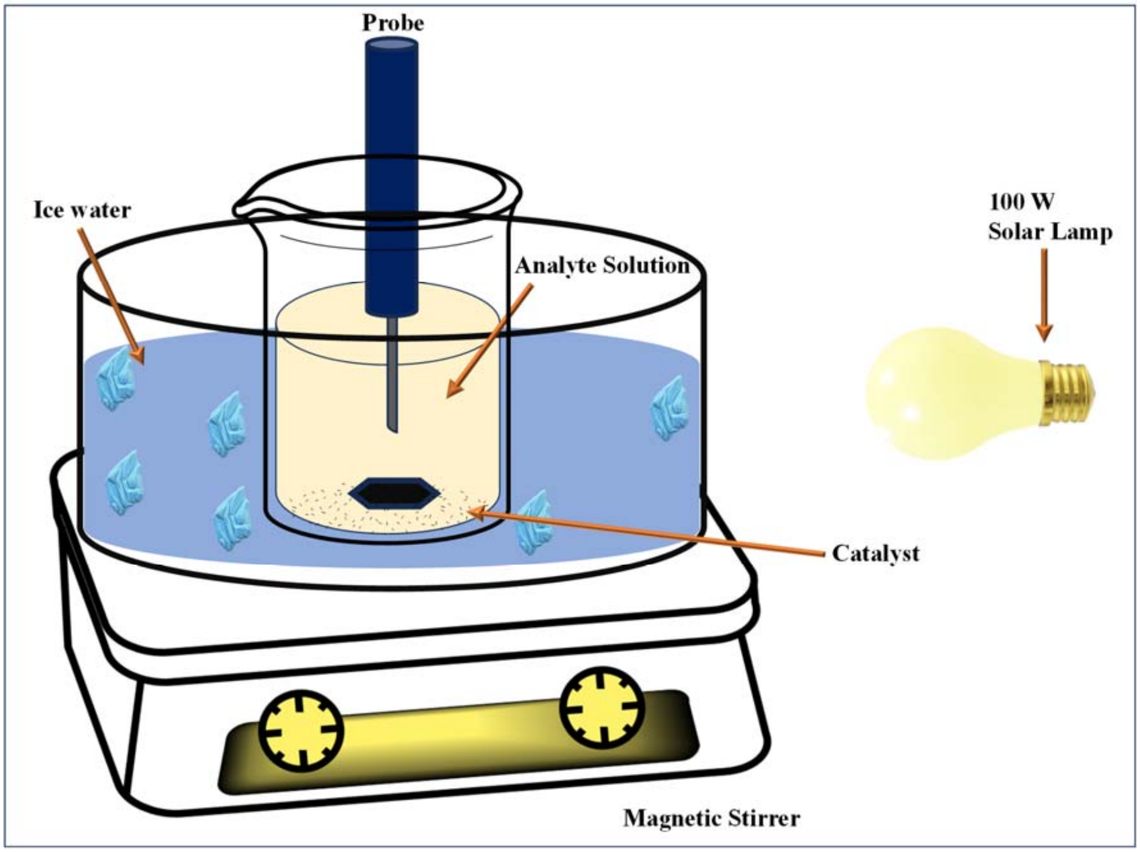

Figure S1: Piezo-photocatalysis of CIP setup arrangement.

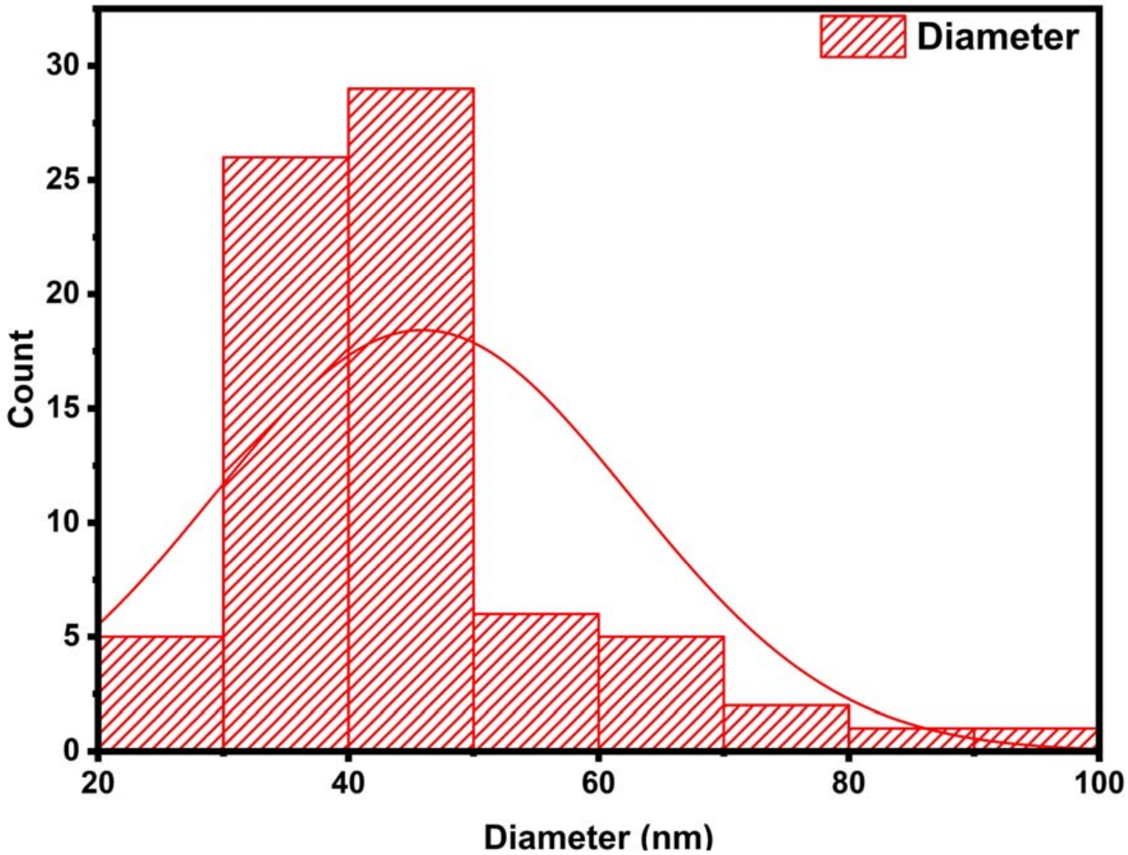

Figure S2: Average diameter of 1.0BTO/CZS nanorods.

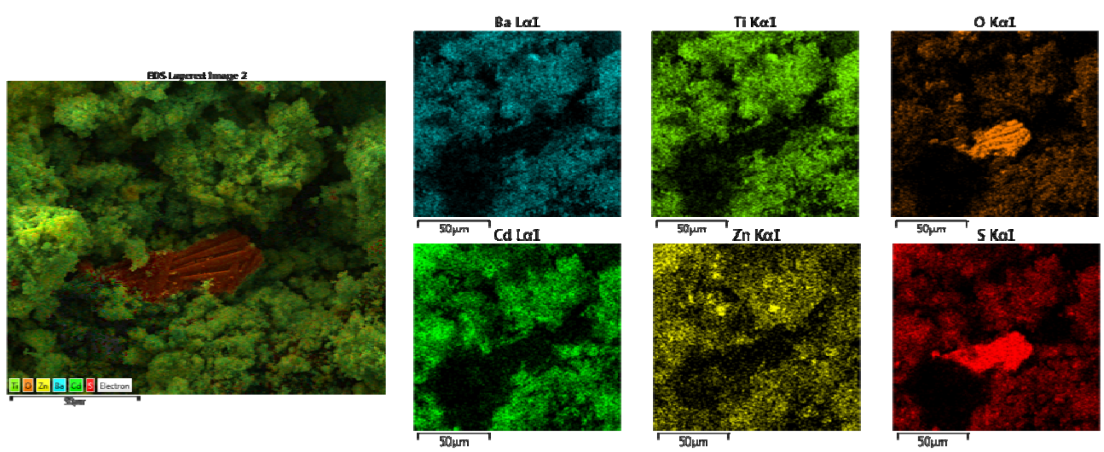

Figure S3: EDS elemental mapping of BTO/CZS

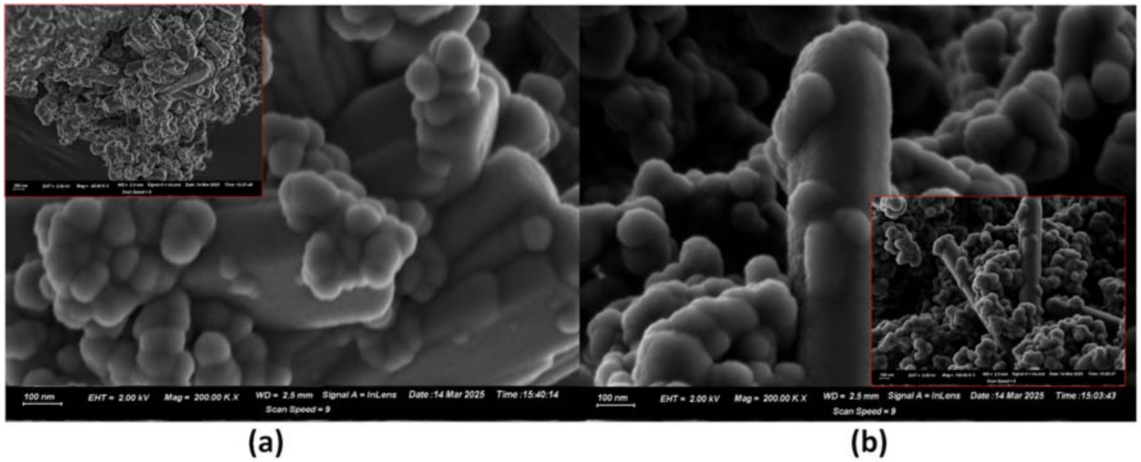

Figure S4: SEM micrograph of (a) 2.0BTO/CZS (insert: 100 nm magnification) and (b) 4.0BTO/CZS (insert: 100 nm magnification)

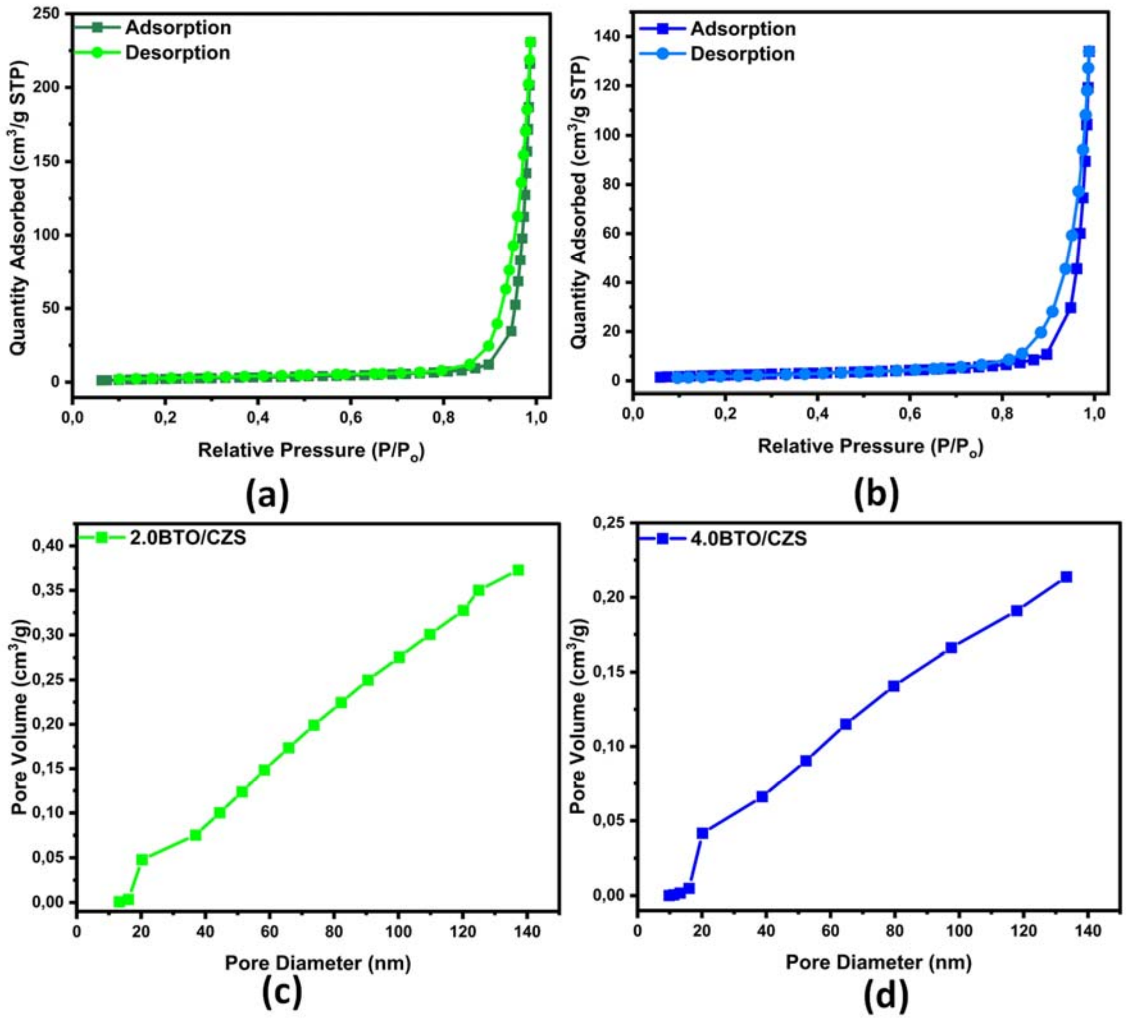

Figure S5: Pore structure analysis of 2.0BTO/CZS and 4.0BTO/CZS. (a-b) N_2 Adsorption-desorption isotherms and (c-d) pore size and volume distribution plots.

Table S1: Pore Size of fabricated nanomaterials.

	Adsorption average pore diameter (BET) (nm)	Desorption average pore diameter (BET) (nm)	BJH Desorption average pore diameter (nm)
BTO	21.1082	21.1082	19.9660
CZS	32.1688	31.2688	30.6664
1.0BTO/CZS	29.2484	29.2484	28.0659
2.0BTO/CZS	148.3974	148.3874	40.8759

4.0BTO/CZS	92.0504	92.0504	36.4546

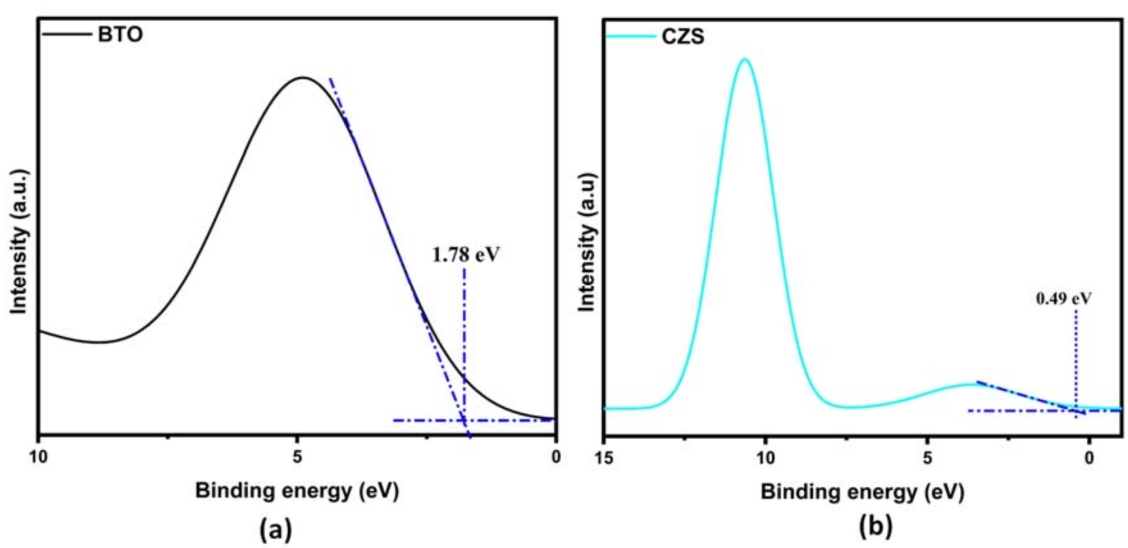

Figure S6: Valence band maxima of (a) CZS and (b) BTO.

Table S2: Transient Photocurrent, piezocurrent, and piezo-photocurrent of BTO, CZS, 1.0BTO/CZS, 2.0BTO/CZS, and 4.0BTO/CZS.

Catalyst	**Transient Photocurrent Response (mA/cm^2)**	**Transient Piezocurrent Response (mA/cm^2)**	**Transient Piezo-Photocurrent Response (mA/cm^2)**	**Band Gap Energy (eV)**
BTO	0.005	0.086	0.128	2.87
CZS	0.176	0.053	0.175	2.20
1.0BTO/CZS	0.505	0.105	1.018	1.87
2.0BTO/CZS	0.380	0.119	0.806	1.89
4.0BTO/CZS	0.102	0.075	0.128	2.03

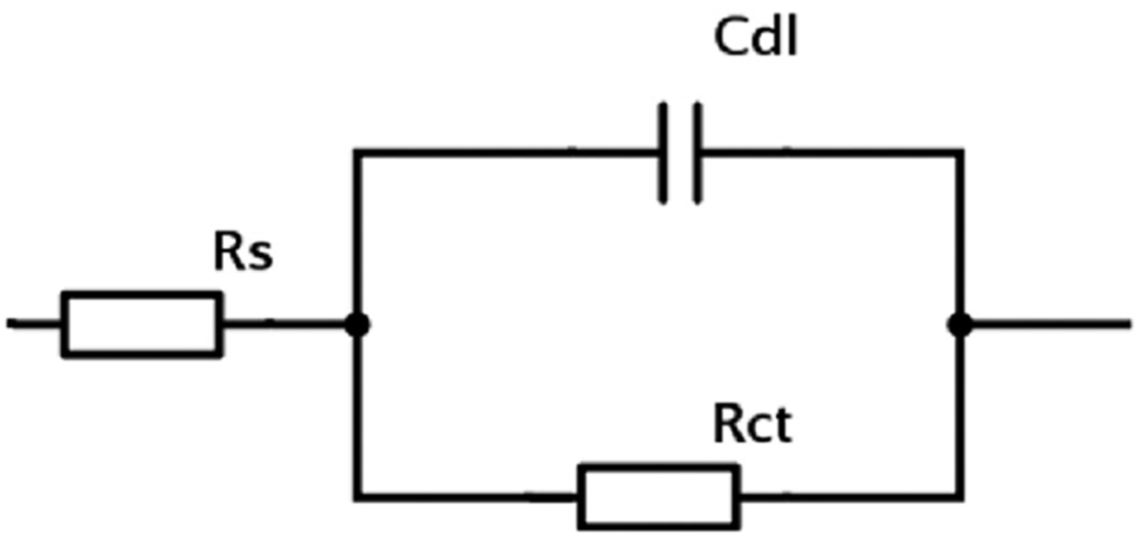

Figure S7: Randles Circuit for EIS fitting.

Table S3: EIS and Mott-Schottky analysis of BTO, CZS 1.0BTO/CZS, 2.0BTO/CZS, 2.0BTO/CZS, and 4.0BTO/CZS.

	R_{ct} (Ω)	**R_s (Ω)**	**Flat band Potential (Efb, V vs Ag/AgCl)**

Catalyst			
BTO	62.662	39.022	-0.46
CZS	197.31	38.155	-0.64
1.0BTO/CZS	17.846	46.785	-0.65
2.0BTO/CZS	22.258	25.806	-0.23
4.0BTO/CZS	98.085	33.016	-0.55

Table S4: Degradation kinetics parameters derived from fitted plots.

	Pseudo-first	**Order kinetics**	**Pseudo-second**	**Order kinetics**
Process	**k_1 (min^{-1})**	**R^2**	**k_2 (min^{-1})**	**R^2**
Piezocatalysis	0.0038	0.4785	0.0009	0.4831
Photocatalysis	0.0070	0.7444	0.0024	0.8106
Piezo-photocatalysis	0.0146	0.9645	0.007	0.8820
Piezolysis	0.0002	0.2271	0.00004	0.2305
Photolysis	0.0005	0.8433	0.0001	0.8439

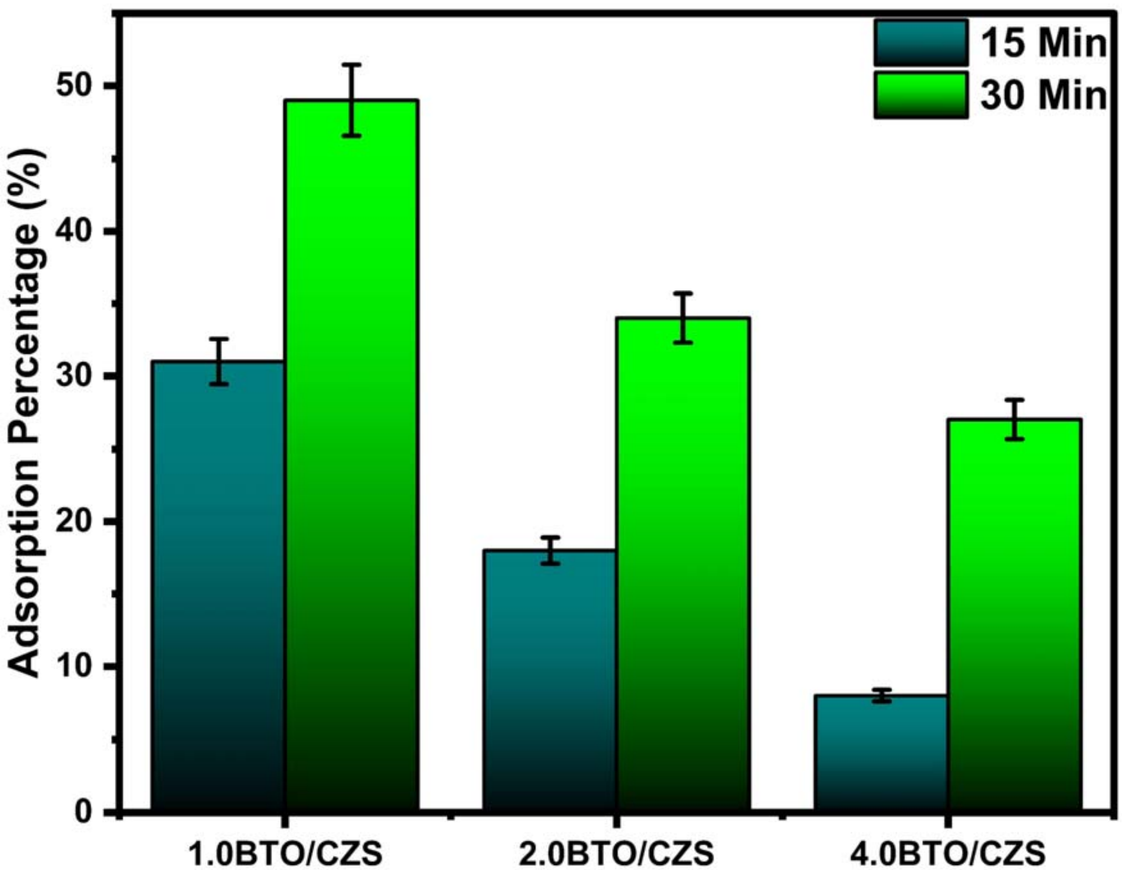

Figure S8: Adsorption efficiency of Composite heterostructures for 15 and 30-minute intervals.

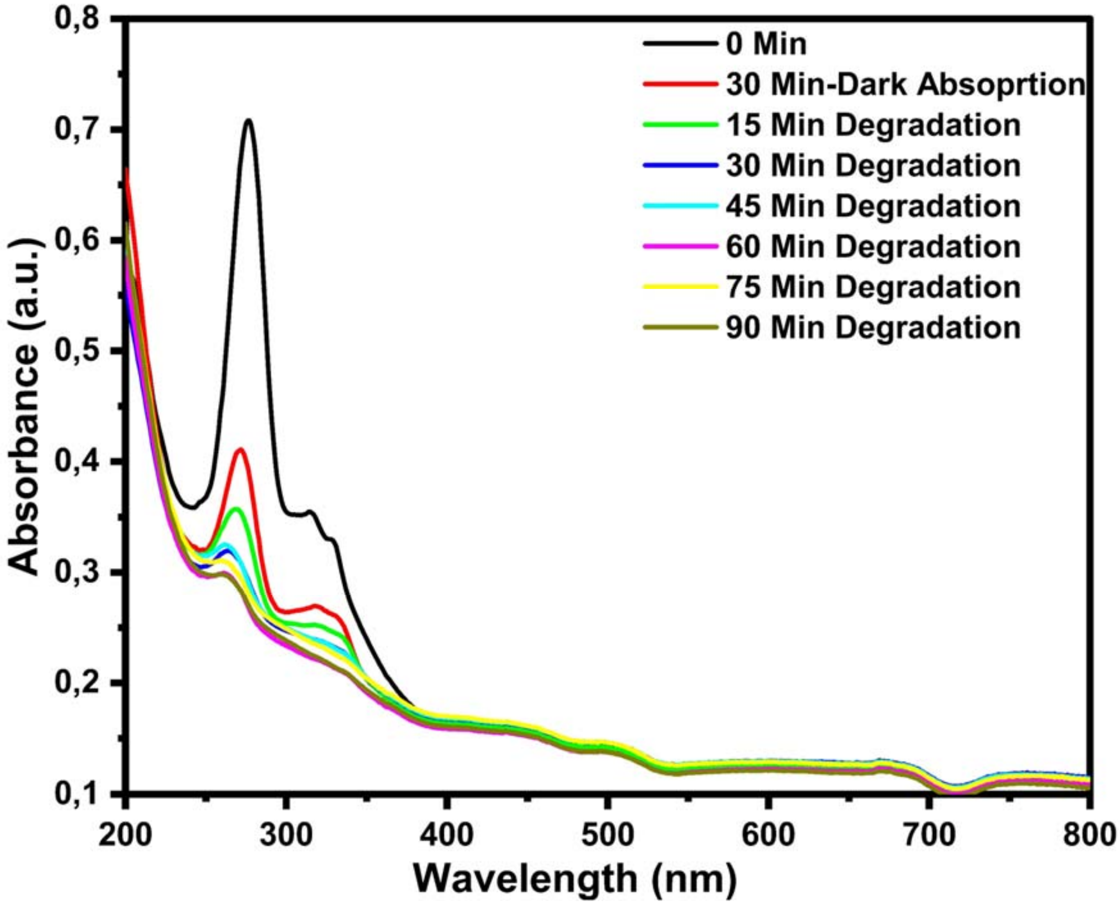

Figure S9: Degradation absorbance of CIP using 1.0BTO/CZS for 90 minutes.

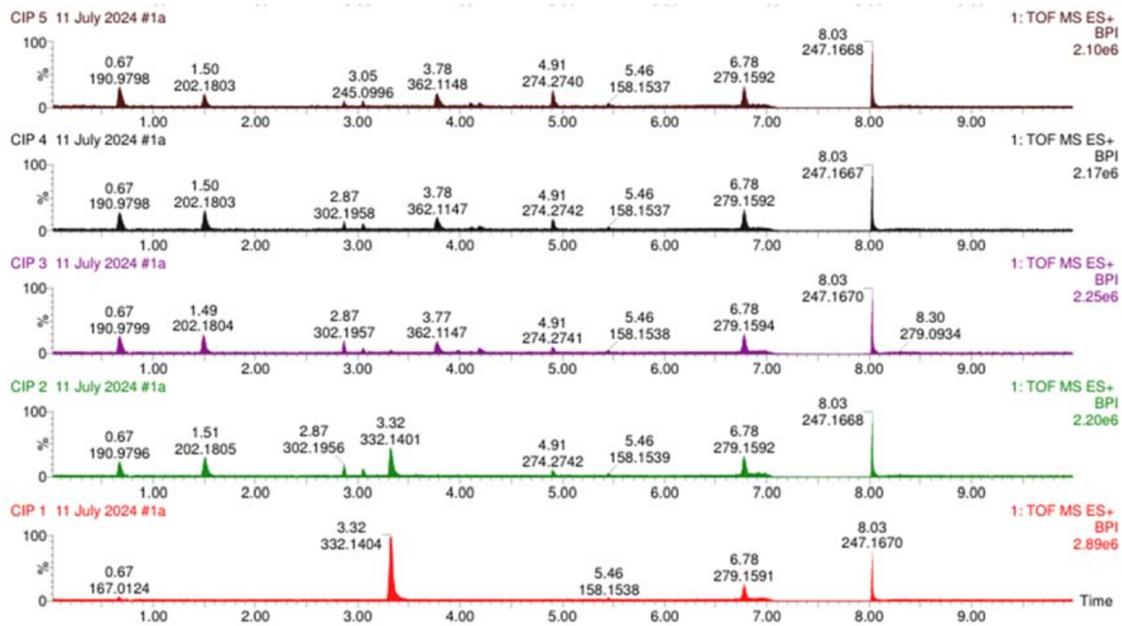

Figure S10: HPLC-MS of CIP during Piezo-Photodegradation (CIP_1: Initial 5ppm sample to CIP-5: Final 90 Minute degradation)

Table S5:

	Bio-Concentration Factor	Oral rat LD_{50}	Developmental toxicity	Mutagenicity
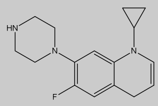	13.21	4046,93	1,09	0,62
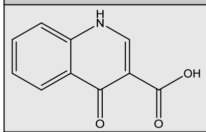	0,81	914,30	0,86	0,08
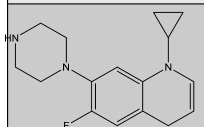	138,66	2940,65	0,74	0,61
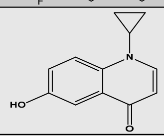	16,59	859,99	0,89	0,22
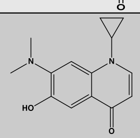	47,71	1145,00	0,90	0,62
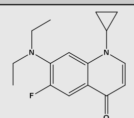	225,73	3220,55	0,76	0,53
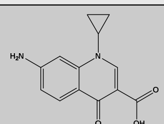	3,35	1848,40	1,04	0,36
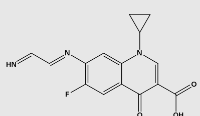	10,60	1585,89	1,04	0,40
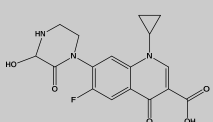	2,92	3958,01	0,79	0,45
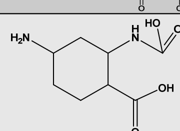	0,0347	3392,05	0,51	0,10

References

[1] Li Y, Li R, Zhai Y, Huang Y, Lee S, Cao J. Improved photocatalytic activity of

BaTiO3/La2Ti2O7 heterojunction composites via piezoelectric-enhanced charge transfer. Appl Surf Sci 2021;570:151146. https://doi.org/10.1016/J.APSUSC.2021.151146.

[2] Masekela D, Hintsho-Mbita NC, Mabuba N. Application of a piezo-photocatalytic thin film (FTO/BaTiO3/SnO2) for enhanced degradation of organic pollutants and disinfection of wastewater. Ceram Int 2023;49:7566–79. https://doi.org/10.1016/J.CERAMINT.2022.10.251.

[3] Chen Z, Li G, Zheng X, Liu Y, Dai J, Huang B, et al. Facile synthesis of advanced BaTiO3/CuPbSbS3 heterostructure photocatalyst with enhanced piezo-photocatalytic degradation performance. Nano Energy 2024;124:109463. https://doi.org/10.1016/J.NANOEN.2024.109463.

[4] Masekela D, Hintsho-Mbita NC, Ntsendwana B, Mabuba N. Thin Films (FTO/BaTiO3/AgNPs) for Enhanced Piezo-Photocatalytic Degradation of Methylene Blue and Ciprofloxacin in Wastewater. ACS Omega 2022;7:24329–43. https://doi.org/10.1021/ACSOMEGA.2C01699/ASSET/IMAGES/LARGE/AO2C01699_0008.JPEG.

[5] Thangavel S, Pazhamalai P, Krishnamoorthy K, Sivalingam Y, Arulappan D, Mohan V, et al. Ferroelectric-semiconductor BaTiO3–Ag2O nanohybrid as an efficient piezo-photocatalytic material. Chemosphere 2022;292:133398. https://doi.org/10.1016/J.CHEMOSPHERE.2021.133398.

[6] Fazli A, Zakeri F, Khataee A, Orooji Y. A BaTiO3/WS2 composite for piezo-photocatalytic persulfate activation and ofloxacin degradation. Commun Chem 2022 51 2022;5:1–14. https://doi.org/10.1038/s42004-022-00707-2.